Section 6.5 (e) on Proximity Effect at low ω PhL 6.21.14

This was installed around June 21, but will probably be rewritten once again soon.

// Yes, it was heavily rewritten. Below is a *very* early version of Section 6.5 (e) ! My bogus low loss model with ω_c is still alive at this point. I see that I was blaming a lot on the "capacitor problem" not being valid at low ω, but I no longer think that is an issue. I really never liked this version of this section 6.5 (e) ! Very unconvincing. (10.8.14)

(e) The Proximity Effect At Low Frequencies

Validity of The Theory at Low Frequencies

The development presented above and leading to the current density plots like Fig 6.12 involves the merging of three pieces of theory:

1. The bipolar-coordinates theory leading to n(θ) for the two cylinder geometry
2. Transmission line theory as presented in Chapters 4 and 5
3. Theory of the fields in a round wire as presented in Appendix D.

Item 1 involves the solution of the electrostatics problem of two parallel cylinders and thus does not involve frequency ω. We therefore expect Item 1 to be just fine at "low frequency".

Item 2 involves the "electro-quasi-static" model for dealing with transmission lines. Contrary to what that phrase intuitively suggests, we have shown that this model is valid for high frequencies and is known to be invalid at low frequencies. For example, we had trouble in Fact 2 of (3.7.4) trying to prove that φ = constant on a transmission line conductor at low frequencies due to the effect of transverse components of the vector potential. Perhaps more significantly, we showed that the assumption that the W(z) difference is independent of the transverse locations of $\mathbf{x}_1$ and $\mathbf{x}_2$ on the conductors is blatantly invalid at low frequencies. This is illustrated in Fig 3.6b which shows that the conductors are *not* equipotentials of A_z at DC (or at low frequencies near DC). The bottom line is that we don't expect Item 2 of the theory to be valid all the wave from high frequencies down to DC.

Item 3 also has subtle problems at low frequencies. The basic ansatz of Appendix D is that all non-power/energy quantities relating to the inside of the wire have time and z dependence given by $e^{j(\omega t-\beta_d z)}$ as shown for the E field in (D.1.1). For a lossless conductor, β_d really is the (real) wavenumber of the dielectric as its name suggests. Since Appendix D assumes a vacuum dielectric (G = 0, but see Section D.9 (d)), lossless here refers only to the effect of conductor resistance. We know that low loss means high σ and therefore small $\delta = \sqrt{2/(\omega\mu\sigma)}$, so for a given σ we associate low loss with high frequency. If we try to incorporate small losses, we can use the loss model of Section D.11 (b) where we end up replacing $\beta_d = \omega/v_d$ (no loss) with $\beta_d = (\omega - j\omega_c)/v_d$ (small loss). A review of Appendix D shows no assumption being made about β_d being real, so the solutions are valid as well for β_d being complex. If we blindly use this lossy expression for β_d as $\omega \rightarrow 0$, we obtain $\beta_d \approx -j\,\omega_c/v_d$ and then $e^{j(\omega t-\beta_d z)}$ gives a exponentially decaying amplitude as z increases. It is "all decay and no wave". We would expect such a decaying amplitude for V(z) along with $q(z) = q(0)\, e^{-j\beta_d z}$ from (4.3.8). But the corresponding $i(z) = i(0)\, e^{-j\beta_d z}$

from (4.9.2) seems peculiar, since with G = 0 we expect to have no decay in the current along the line. At DC the inductance and capacitance of the line have no effect and the model becomes just the conductor resistance, as suggested by this DC version of Fig K.1

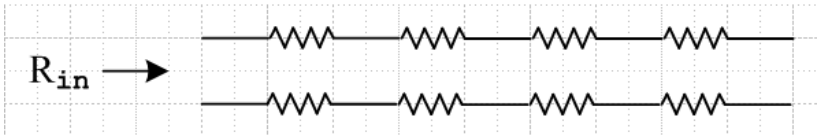

This issue is partially resolved by noting that Appendix D applies only to an infinite transmission line, and then the above network model gives $R_{in} = \infty$ so i(0) = 0. We note that the low loss model just mentioned makes use of the transmission line equations in its derivation, and these equations are known to be invalid at low frequencies for the reasons given above in Item 2, so we don't really expect our loss model to be valid near ω = 0.

Appendix D has other low frequency problems as well. For example, the charge pumping boundary condition (D.2.23) says $J_r(r=a-\varepsilon,\theta) = j\omega\ n(\theta)$. We then assume that $J_r = \sigma E_r$ and this then becomes a condition on the E_r field: $E_r(r=a-\varepsilon,\theta) = (j\omega/\sigma)\ n(\theta)$. We then use this boundary condition with our Helmholtz equation E field solutions to determine the constants K_m and a_m and thus to obtain the E field results shown in (D.2.33). However, we know that at DC (and presumably near DC), the radial Hall effect exists as outlined in Section N.7. At DC we learn that in a round wire there is a Hall field $E_r = E_s\ (r/a)$ from (N.7.12), while at the same time $J_r \equiv 0$ from (N.7.11). This last result is consistent with the boundary condition just quoted $J_r(r=a-\varepsilon,\theta) = j\omega\ n(\theta)$ as $\omega \rightarrow 0$, but our assumption that $J_r = \sigma E_r$ at low frequency is seen to be grossly invalid. Normally one thinks of the radial Hall effect as a miniscule effect, but at low frequencies all the transverse fields in a round conductor are miniscule so the Hall field becomes significant. Moreover, Appendix D assumes no free charge density inside the conductor, but there is a small free charge near ω = 0 due to this same Hall effect. There is also a Hall surface charge that Appendix D ignores.

To summarize our Item 3 conclusions, the results (D.2.33) which we have used above to make plots of the conductor current densities are expected to be invalid at low frequencies.

It is not obvious just how low ω can be for the fields (D.2.33) to remain valid. For sure they are not valid in the immediate vicinity of ω = 0, so we cannot use these field expressions to study the limit $\omega \rightarrow 0$, and this will be illustrated below. We expect that the lower bound for ω will depend on the transmission line geometry. As a ballpark guess we might consider this lower bound on ω to be the ω_c parameter mentioned above. We show in the two Examples of Section D.11 that f_c = 7.7 KHz for Belden 8281 coaxial cable, whereas f_c = 5.5 Hz for a typical power transmission line.

Proximity Effect at Low Frequency

To review, in various places in the above analysis, it was assumed that ω is high enough to put the transmission line in either the strong or extreme skin effect regime of (3.7.3) which roughly means $\delta < a/10$. In order to base the analysis on "the capacitor problem" as we have done (the electro-quasi-static model), we had to avoid the low frequency range which, expressed in terms of skin depth δ, is roughly $a/10 < \delta < \infty$. Only then could we be assured that φ = constant *and* A_z = constant on the conductor surfaces as declared in (3.7.4) and (3.7.20), and only then are the transmission line equations and

parameter evaluations of Chapter 4 valid. Our analysis of the proximity effect presented above inherits all these assumptions (in addition to the requirement of being in the transmission line limit so $\lambda >> a$).

As described in the text section below (3.7.21), we might blindly assume that our transmission line theory is "ballpark valid" in the low frequency range, and then the proximity effect calculation as given above would also apply approximately. For example, if we use our program above with a = 10 and $\delta = 10$, which is deep into the low frequency range, the plots look like this for $\xi_1 = -3$:

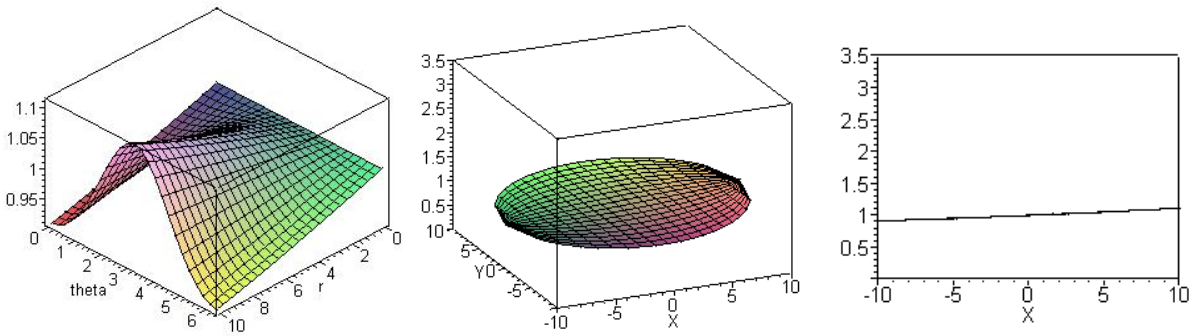

$|J_z|$ Distribution in left round wire for a = 10, $\delta = 20$ and $\xi_1 = -3.00$ Fig 6.16

The current distribution $|J_z|$ shown on the right is a flat disc which is almost horizontal but still has a very slight proximity effect visible in the right view. Since $\xi_1 = -3$ in this example, the conductors are "far apart", and we certainly expect intuitively to see a nearly flat $|J_z|$ distribution as we would see at DC ($\omega = 0$, since no eddy currents).

However, if we instead use $\xi_1 = -1.00$, the program gives a strong proximity effect even if we lower the frequency way down to $\delta = 200$ (and a = 10),

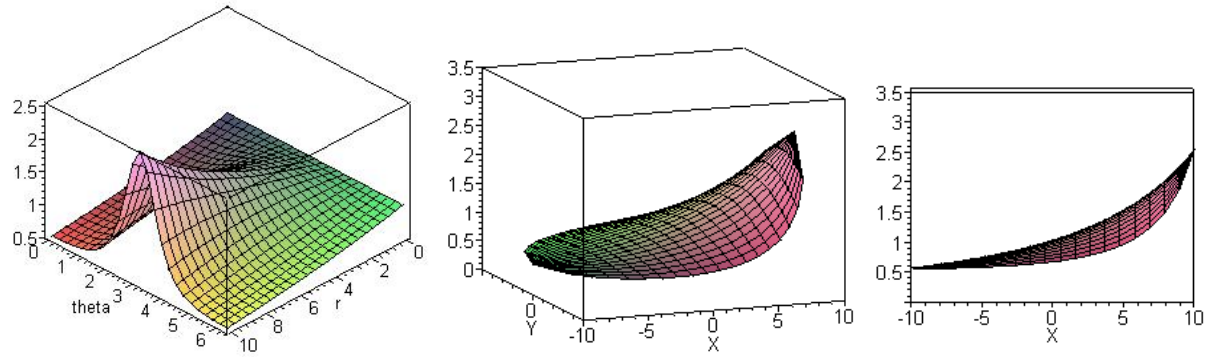

$|J_z|$ Distribution in left round wire for a = 10, $\delta = 200$ and $\xi_1 = -1.00$ Fig 6.17

Even at a very low frequency, the strongly peaked capacitor's $n(\theta)$ is maintained and "gets into" the $|J_z|$ distribution. This result is incorrect based on one's expectation that J_z is "uniform at DC", so for the last example, our model blindly stretched to low ω gives a wrong result. We summarized in the previous subsection why we expect the model to be wrong.

There is an escape hatch (already alluded to in the above network picture) which sheds some light on this paradoxical limit as $\omega \to 0$. In the eddy current analysis of Section P.8, the two parallel cylinders considered there carry current I and -I. But our proximity effect described above is for a properly terminated active transmission line, not two parallel wires that are shorted together at one end. A properly terminated transmission line, which we equate with the infinite transmission line this document addresses, must be terminated by Z_0. If we naively apply our theory as if it were valid at very low ω, we have

$$Z_0 \equiv V/I = \sqrt{\frac{\mathbf{z}}{\mathbf{y}}} = \sqrt{\frac{R + j\omega L}{G + j\omega C}} \quad . \qquad (4.11.16)$$

Appendix D (in particular, the charge pumping boundary condition (D.2.24)) assumes a vacuum dielectric, so conductance G = 0. Thus, in the limit $\omega \to 0$ we find that $Z_0 = \infty$. If we drive this transmission line with V = 10 volts at f = 0.1Hz, we find that $I \approx 0$ and there is no current at all, so the fact that J_z is asymmetric is not relevant.

The conclusion is that our entire theory is only "ballpark accurate" at low ω, and therefore we have no trustworthy conclusions regarding the proximity effect at low frequencies. However, if we incorporate the loss model of Appendix D.11 and go ahead and **blindly assume** "ballpark accuracy" of the Appendix D results at low ω, here is a statement of our conclusions regarding J_z asymmetry:

1. For a well-conducting $\mu=\mu_0$ round wire which is part of a 2-conductor transmission line carrying a traveling wave of the form $e^{j(\omega t - \beta_d z)}$ through a vacuum dielectric, the E fields inside the wire are completely determined by the relative moments η_m of the surface charge distribution $n(\theta)$ as obtained from an electrostatic calculation based on the shape of the line cross section. From (D.2.33) the fields are:

Second summary of the E field solutions : $\quad R_{dc} = \frac{1}{\sigma\pi a^2} \quad \beta'^2 = \beta^2 - \beta_d^2 \qquad (D.2.33)$

$$E_z(r,m) = (1/4)\,\eta_m\, I\, R_{dc}\, (a\beta')\, f_m \qquad f_m = \left[\frac{J_m(x)}{J_{m+1}(x_a)} - \frac{J_m(x)}{J_{m-1}(x_a)}\right] \qquad x = \beta' r$$

$$E_r(r,m) = (j/4)\,\eta_m\, I\, R_{dc}\, (a\beta_d)\, g_m \qquad g_m = \left[\frac{J_{m+1}(x)}{J_{m+1}(x_a)} + \frac{J_{m-1}(x)}{J_{m-1}(x_a)}\right] \qquad x_a = \beta' a$$

$$E_\theta(r,m) = (1/4)\,\eta_m\, I\, R_{dc}\, (a\beta_d)\, h_m \qquad h_m = \left[\frac{J_{m+1}(x)}{J_{m+1}(x_a)} - \frac{J_{m-1}(x)}{J_{m-1}(x_a)}\right]$$

Parameters in the E field expressions are:

a	radius of the wire
σ	conductivity of the round wire
R_{dc}	$= 1/(\pi a^2 \sigma)$ = DC resistance of the round wire per unit length
I	current magnitude in the wire
β_d	wavenumber of the dielectric wave
β	wavenumber inside the conductor
β'	$\beta'^2 = \beta^2 - \beta_d^2$

η_m relative moments of $n(\theta)$, $\eta_m = N_m/N_0$ as in (D.1.5)

where (see App D.11 for the soft cutoff frequency ω_c) ,

$\beta_d = (\omega - j\omega_c)/v_d$ $\omega_c = (v_d^2/2)\,(R'_{dc}C)$ $v_d = c$ = the speed of light
ω = angular frequency of the monochromatic wave
R'_{dc} = total resistance per unit length of both conductors.
C = capacitance per unit length of the two conductors
$\beta = e^{j3\pi/4}\,(\sqrt{2}/\delta) = (j-1)/\delta$ $\delta \equiv \sqrt{2/\omega\mu_0\sigma}$ = skin depth (6.5.21)

2. At all frequencies, including the limit $\omega \to 0$ (where $Z_0 \to \infty$), the current distribution J_z in the wire is non-uniform, and is determined from $J_z = \sigma E_z$. The current is non-uniform because the amplitudes of the partial-wave fields $E_z(r,m)$ for $m \neq 0$ do not in general vanish -- see for example (D.11.17,18). The one exception occurs if the round wire is the center conductor of a coaxial cable (see Chapter 2). See Appendix D.10 and D.11 for discussion of the high and low frequency limits of the boxed E fields above.

3. These conclusions apply to an infinite transmission line, or to a truncated transmission line which is properly terminated by $Z_t = Z_0$ where Z_0 is given by (4.4.12) with G = 0 (since vacuum dielectric). The conclusions do not apply to a truncated transmission line which is terminated with some fixed impedance at all ω, such as $Z_t = 0$.

We know that for the problem of two parallel cylindrical conductors (or any uniform parallel conductors) which carry I and -I and are shorted at one end, J_z is uniform at DC. We know this because at $\omega = 0$ there are no eddy currents induced by one wire into the other. The DC B field of wire #2 has no influence on the current density J_z in wire #1, though it does induce a tiny Hall charge onto the surface of wire #1 and a corresponding transverse Hall E field since the B field of wire #2 temporarily deflects electrons in wire #1 (see Appendix N for various Hall examples). This deflection effect is mentioned in the text below Fig P.12 in Appendix P. In any event, if the DC B field of wire #2 does not affect J_z in wire #1, then J_z in wire #1 doesn't even know that wire #2 is present, so wire #2 could just as well be removed. The isolated wire #1 then if round (Chapter 2) would have a uniform J_z certainly with no proximity effect.

It would be reassuring if our transmission line model could account for the gradual transition from low ω to $\omega = 0$ where the asymmetric J_z smoothly approaches a uniform a J_z. Unfortunately, our model only applies to an infinite (or properly terminated) transmission line, and thus cannot expose the $\omega \to 0$ limit for parallel conductors terminated in a fixed load. One can superpose a left- and right-going Appendix D wave solution to get a standing wave situation to model the shorted cylinder pair, but since the Appendix D solutions are themselves not valid at low ω, this does not resolve the problem.

In a proper treatment of the fixed-load problem, as $\omega \to 0$ one would see the eddy currents gradually decrease, one would arrive at a DC current I, and one would have $J_z \to$ uniform. The problem with our transmission line model is that, for the infinite line, or one in which the termination is constantly increased to equal Z_0, as $\omega \to 0$ the eddy currents *do* gradually vanish, but *so does* the J_z associated with the current I, so the ratio of these currents maintains the asymmetric pattern of Fig 6.17.

A solution of the fixed load two-cylinder problem could be based on the eddy current methods outlined qualitatively in Appendix P and is no doubt available somewhere in the literature. This solution would then show the proximity and skin effects gradually vanishing as $\omega \rightarrow 0$, leaving a uniform J_z.